Recovery of a reversed phase sequence in one ternary liquid-crystal-mixture system

Shun Wang,[1] LiDong Pan,[1] B. K. McCoy,[1,2] S. T. Wang,[3] R. Pindak,[3] H. T. Nguyen,[4] and C. C. Huang[1]
[1]*School of Physics and Astronomy, University of Minnesota, Minneapolis, Minnesota 55455, USA*
[2]*Department of Mathematics and Physics, Azusa Pacific University, Azusa, California 91702, USA*
[3]*NSLS, Brookhaven National Laboratory, Upton, New York 11973, USA*
[4]*Centre de Recherche Paul Pascal, CNRS, Université Bordeaux I, Avenue A. Schweitzer, F-33600 Pessac, France*
(Received 19 September 2008; revised manuscript received 17 November 2008; published 26 February 2009)

The *n*OHFBBB1M7 ($n=10$) compound, 10OHF, shows a reversed SmC^*_{FI2}-SmC^* phase sequence, unique among all known antiferroelectric liquid crystals. This reversed phase sequence is stabilized when 10OHF is doped with 9OTBBB1M7(C9) or 11OTBBB1M7(C11). In contrast, doping of the homologous members ($n=9$, 11, or 12) eliminates the SmC^*_{FI2} phase. One 10OHF/11OHF mixture without the SmC^*_{FI2} phase was selected for further studies. By adding C9 into this particular mixture, the reversed phase sequence is revived. To our surprise, even though 11OHF destabilizes the SmC^*_{FI2} phase in binary mixtures with 10OHF, it significantly increases the SmC^*_{FI2} temperature range in the 10OHF/11OHF/C9 ternary mixtures.

DOI: 10.1103/PhysRevE.79.021706 PACS number(s): 61.30.Gd, 64.70.M−, 77.84.Nh

I. INTRODUCTION

Since the discovery of chiral smectic liquid crystal phases [1,2], extensive scientific research has been focused on investigating the structure of the variants of chiral smectic-*C* (SmC^*) phases and aimed to gain better understanding of the underlying physical reasons for the formation of these phases. To date, optical experiments [3,4] and resonant x-ray diffraction (RXRD) [5] have successfully elucidated the interlayer orientational arrangement of the SmC^* variant phases. In SmC^* variant phases, elongated molecules form a layered structure. In the layer plane, molecules have liquid-like ordering. Within the layers, molecular axes are tilted along a common direction, with an angle relative to the layer normal and an azimuthal orientation. Different SmC^* variant phases are distinguished by the azimuthal arrangements of molecular orientations among layers. In the smectic-C^*_α (SmC^*_α) phase and the SmC^* phase, the molecular orientation forms a helical structure. In the SmC^*_α phase, the helical pitch is on the order of 10 layers. The SmC^* phase has a longer pitch, usually several hundred layers. Without change in symmetry, the SmC^*_α-SmC^* transition is a first-order transition ending at a critical point [6]. The smectic-C^*_{FI2} (SmC^*_{FI2}) and smectic-C^*_{FI1} (SmC^*_{FI1}) have four- and three-layer unit cells, respectively, which are best described by the distorted clock model [7,8]. In the antiferroelectric smectic-C^*_A (SmC^*_A) phase, the tilt orientation alternates between adjacent layers [2].

Among antiferroelectric liquid crystal compounds, a typical order of appearance of mesophases on cooling is the following: Sm*A*-SmC^*_α-SmC^*-SmC^*_{FI2}-SmC^*_{FI1}-SmC^*_A, with some of these phases missing in many compounds. Laux *et al.* [9] reported a unique phase sequence SmC^*_α-SmC^*_{FI}-SmC^* upon cooling in *n*OHFBBB1M7 ($n=10$), 10OHF. Wang *et al.* [10] identified the phase sequence of 10OHF to be SmC^*_α-SmC^*_{FI2}-SmC^*. It was demonstrated by Sandhya *et al.* [11] that the SmC^*_{FI2} phase was thermodynamically monotropic and only appeared upon cooling. They also showed that the SmC^*_{FI2} phase was unstable under bias voltage. It was found that in binary mixtures of 10OHF and *n*OTBBB1M7 ($n=9$), C9, the SmC^*_{FI2} temperature window expanded rapidly with increasing concentration of C9 and the SmC^*_{FI2} phase became enantiotropic [10,11]. Binary mixtures of 10OHF and C11 showed similar behavior. The SmC^* phase found in both compounds was squeezed out and the SmC^*_{FI2} phase was stabilized. The phase reversal phenomenon has also been observed in other liquid crystal compounds [12]. The other homologs of 10OHF (namely, 9-, 11- and 12OHF) do not show reversed phase sequence behavior [13]. In this paper, we employed null transmission ellipsometry (NTE) to investigate samples of 10OHF doped with its homologs. The result shows that the reversed phase sequence disappeared with moderate dopant concentrations. For further study, we select the 73% 10OHF/27% 11OHF binary mixture, which does not show the SmC^*_{FI2} phase. By adding C9 into this particular mixture, the reversed phase sequence is revived. For a given concentration of C9, in the ternary 10OHF/11OHF/C9 mixtures, SmC^*_{FI2} temperature windows are found to be larger than in the corresponding 10OHF/C9 binary mixtures.

II. EXPERIMENTAL METHODS

The detailed experimental setup of NTE is described elsewhere [14]. Freestanding film geometry is used in the system. A small electric field (**E**), on the order of 1 V/mm, is applied in the film plane to align the net polarization of the film. The **E** orientation with respect to the laser's plane of incidence is denoted by an angle α. Ellipsometric parameters Δ and Ψ are measured as a function of α and temperature. Δ is the phase difference between the $\hat{p}$ and $\hat{s}$ components of the incident light necessary to produce linearly polarized transmitted light. Ψ denotes the orientation of the polarization of the transmitted linearly polarized light.

RXRD experiments were conducted at National Synchrotron Light Source. The incident x-ray energy was tuned to $E_0=2.471$ keV, near the K_α absorption edge of sulfur. Freestanding films were prepared in a temperature controlled oven, flushed with helium. Diffraction with momentum transfer along the layer normal (**z**) was done to characterize

 ©2009 The American Physical Society

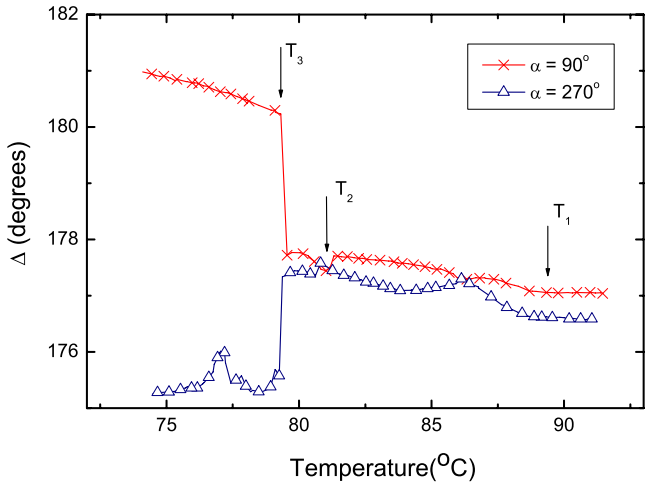

FIG. 1. (Color online) Δ as a function of temperature for a 56-layer film of 75% 10OHF/25% 11OHF mixture from NTE while cooling at 0.1 °C/min. α is the angle between the **E** orientation and the incident plane of the laser light.

the molecular arrangements in various smectic phases. The associated wave-vector transfer (Q_z) is measured. The locations of the resonant and Bragg peaks give the size of the repeated units of the SmC^* variant phases. The detailed experimental setup can be found in Ref. [5].

III. RESULTS

We have studied three mixtures of 10OHF/9OHF (15%, 29% and 50% of 9OHF) and three mixtures of 10OHF/11OHF (15%, 25% and 27% of 11OHF). Figure 1 illustrates the ellipsometric parameter (Δ_{90}, Δ_{270}) obtained from an NTE temperature scan of a 56-layer film of 75% 10OHF with 25% 11OHF at α=90° and α=270°. The small difference between Δ_{90} and Δ_{270} above T_1 is due to surface ordering in the SmA phase. The oscillations of Δ_{90} and Δ_{270} between T_1 and T_2 are signatures of the SmC^*_α phase [15]. Between T_2 and T_3 is the SmC^*_{FI2} phase. At T=80 °C the ellipsometric parameters Ψ and Δ were obtained as a function of α. The data show that Ψ and Δ have 180° symmetry, which is the characteristic of the SmC^*_{FI2} phase [4]. Below T_3 the large span of Δ between α=90° and α=270° is the feature of the SmC^* phase [16]. The phase sequence of this mixture upon cooling is SmA (89.0 °C) SmC^*_α (81.1 °C) SmC^*_{FI2} (79.7 °C) SmC^*.

A phase diagram of 10OHF/9OHF and 10OHF/11OHF mixtures is shown in Fig. 2. The SmC^*_{FI2} phases in all the mixtures are monotropic. The temperature window of the SmC^*_{FI2} phase decreases with increasing 9OHF concentration. There is no SmC^*_{FI2} phase observed in the 50% 9OHF/50% 10OHF mixture. The stability of the SmC^*_{FI2} phase increases slightly with 10% 11OHF doping. However, for 25% 11OHF doping, the temperature window of the SmC^*_{FI2} phase decreases dramatically to 1.4°. For the 73% 10OHF/27% 11OHF mixture, the SmC^*_{FI2} phase completely disappeared. We have also done studies on 10OHF/12OHF mixtures. Similar to 10OHF/11OHF mixtures, the SmC^*_{FI2} phase disappears near 25% dopant concentration.

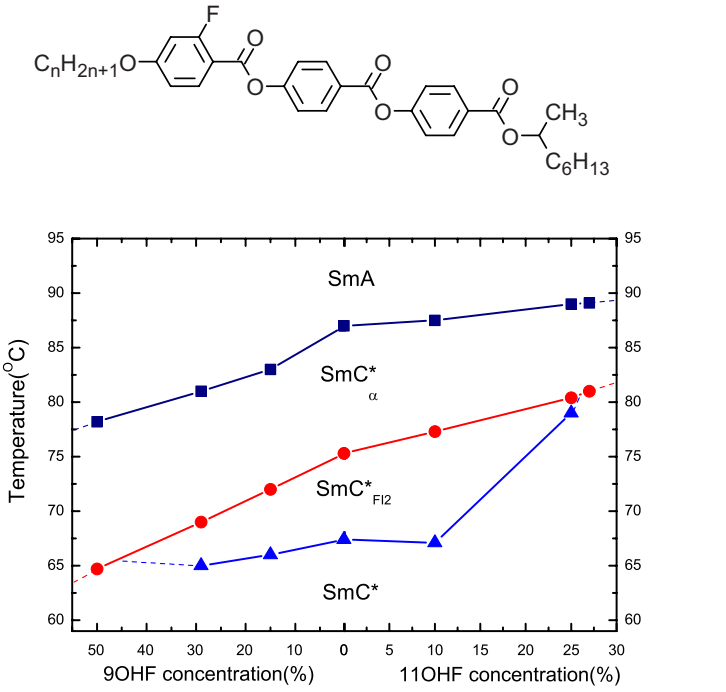

FIG. 2. (Color online) Phase diagram of $10OHF_{1-u}$, $9OHF_u$, and $10OHF_{1-v}$ $11OHF_v$ mixtures. On the top is the chemical structure of nOHFBBB1M7(nOHF). The phase sequences of 9OHF and 11OHF are SmA (63 °C) SmC^*_α (52 °C) SmC^* and SmA (94 °C) SmC^*_α (89 °C) SmC^*.

The absence of the SmC^*_{FI2} phase in the 73% 10OHF/27% 11OHF mixture makes it a very good candidate for further study on the reversed phase sequence. Experiments have been done on binary mixtures of 9-, 11- and 12OHF with C9. The phase reversal phenomenon is not observed. It shows this reversed phase sequence is indeed a unique property of 10OHF. It is intriguing to investigate whether or not and where the SmC^*_{FI2} phase will reappear by adding C9 into this 73% 10OHF/27% 11OHF mixture.

A series of $(73\%\ 10OHF/27\%\ 11OHF)_{1-x}$ $C9_x$ mixtures with x=0.10, 0.15 and 0.25 were prepared and investigated by using NTE. Figure 3 shows the phase diagram of $(73\%\ 10OHF/27\%\ 11OHF)_{1-x}$ $C9_x$ mixtures obtained from NTE measurements. The phase sequence at x=0.15 was confirmed by RXRD studies. For example, at T=83.6 °C, the resonant peak is at Q_z/Q_0=1.17 ($Q_0=2\pi/d$ and d is the layer spacing), indicating the SmC^*_α phase with a pitch value of 5.8 layers. At T=73 °C, the resonant peak position near Q_z/Q_0=1.25 reveals a four layer structure. This proves that it is the SmC^*_{FI2} phase. At T=52.6 °C, a resonant peak on the shoulder of the (002) Bragg peak is observed. It is the SmC^* phase with a pitch of 150 layers.

The effect of C9 doping on pure 10OHF is that it stabilizes the SmC^*_{FI2} phase existing in 10OHF. In the 73% 10OHF/27% 11OHF binary mixture, there is no SmC^*_{FI2} phase. By adding 10% C9 into this binary mixture, the SmC^*_{FI2} phase is restored with a temperature window of 22°, which is just slightly smaller than 24° found in pure C9. In addition, the SmC^*_{FI2} phase range expands to more than 30° with increasing C9 concentration in the ternary mixtures.

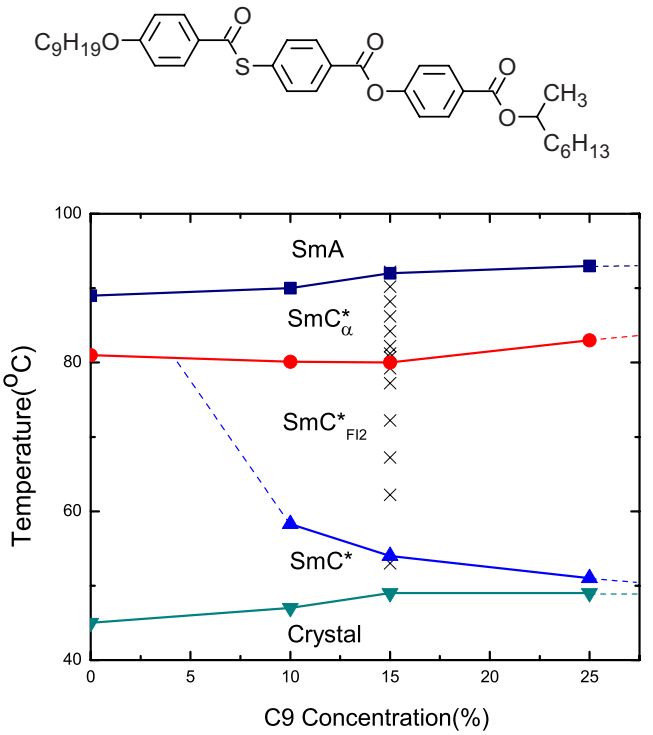

FIG. 3. (Color online) Phase diagram of $(73\%\ 10\mathrm{OHF}/27\%\ 11\mathrm{OHF})_{1-x}\ \mathrm{C9}_x$ mixtures. The crosses mark the temperatures at which RXRD was performed. On the top is the chemical structure of 9OTBBB1M7(C9). The phase sequence of C9 is Sm*A* (115 °C) $\mathrm{Sm}C^*_\alpha$ (109 °C) $\mathrm{Sm}C^*_{FI2}$ (85 °C) $\mathrm{Sm}C^*_A$. The disappearance of the $\mathrm{Sm}C^*_\alpha$-$\mathrm{Sm}C^*_{FI2}$ transition below 10% C9 mixture is not an important issue for this paper. Without any data in this range, we represent this part of phase boundary by a dashed line.

The $\mathrm{Sm}C^*_{FI2}$ phase becomes enantiotropic. Meanwhile, the temperature window of the SmC^* phase is reduced dramatically with C9 doping.

It is interesting to compare the $\mathrm{Sm}C^*_{FI2}$ phase temperature window of $(73\%\ 10\mathrm{OHF}/27\%\ 11\mathrm{OHF})_{1-x}\ \mathrm{C9}_x$ mixtures with that of the 10OHF/C9 mixtures. Since pure 11OHF has no $\mathrm{Sm}C^*_{FI2}$ phase and it destabilizes the $\mathrm{Sm}C^*_{FI2}$ phase when mixing with 10OHF, one might expect that 11OHF would also decrease the temperature window of the $\mathrm{Sm}C^*_{FI2}$ phase when added into the 10OHF/C9 mixture. Figure 4 shows the temperature range of the $\mathrm{Sm}C^*_{FI2}$ phases in the 10OHF/C9 mixtures from Ref. [10] and the ternary mixtures studied in this paper. The data point at 15% C9 for the binary mixture has a larger error bar because we did not study this particular mixture. The data were constructed by interpolation from the 10OHF/C9 phase diagram. Surprisingly, 11OHF broadens the $\mathrm{Sm}C^*_{FI2}$ phase in all the ternary mixtures, by up to 15°.

To gain a better knowledge about this phase reversal phenomenon, we also studied the pitch evolution of the $(73\%\ 10\mathrm{OHF}/27\%\ 11\mathrm{OHF})_{0.85}\ \mathrm{C9}_{0.15}$ mixture in the $\mathrm{Sm}C^*_\alpha$ phase by RXRD, which is shown in Fig. 5(a). Upon cooling, the pitch is found to be 6.7 layers just below the Sm*A*-$\mathrm{Sm}C^*_\alpha$ transition. Then the pitch decreases to 5.6 layers and subsequently increases to 5.9 layers. Unlike in most of the compounds and mixtures we have investigated, the pitch in this ternary mixture evolves nonmonotonically with temperature in the $\mathrm{Sm}C^*_\alpha$ phase.

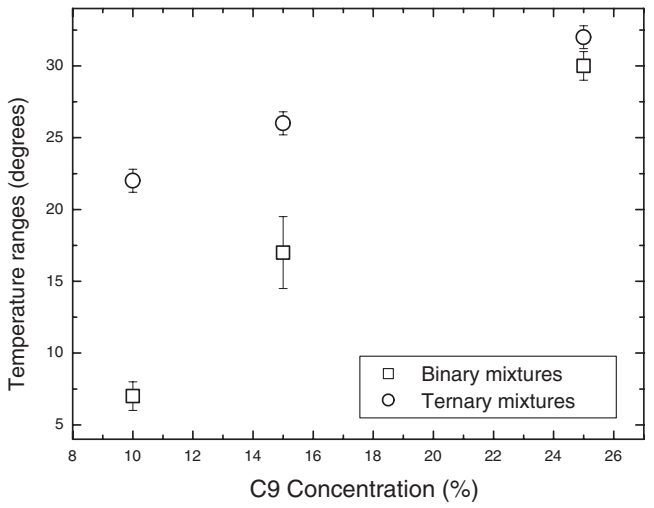

FIG. 4. Temperature ranges of the $\mathrm{Sm}C^*_{FI2}$ phase in the ternary $(73\%\ 10\mathrm{OHF}/27\%\ 11\mathrm{OHF})_{1-x}\ \mathrm{C9}_x$ mixtures and in the binary $(10\mathrm{OHF})_{1-x}\ \mathrm{C9}_x$ mixtures as a function of C9 concentration (x).

To date, several theoretical models predict the existence of the mesophase with six-layer periodicity [17–19]. From Fig. 5(a), we can see the pitch value yields 5.95 layers (our resolution is about ±0.05 layer) at two temperatures with 1° separation before the transition to the $\mathrm{Sm}C^*_{FI2}$ phase. However, the shape of the resonant satellite peaks at these two temperatures did not show any difference from the rest of data taken in the $\mathrm{Sm}C^*_\alpha$ phase [Figs. 5(b)–5(d)]. Our simulation shows that for a distorted six-layer phase, the resonant peaks are split peaks with different intensities. Meanwhile, from the NTE measurements, all the studied films are, within our experimental resolution, optically uniaxial [20] above the

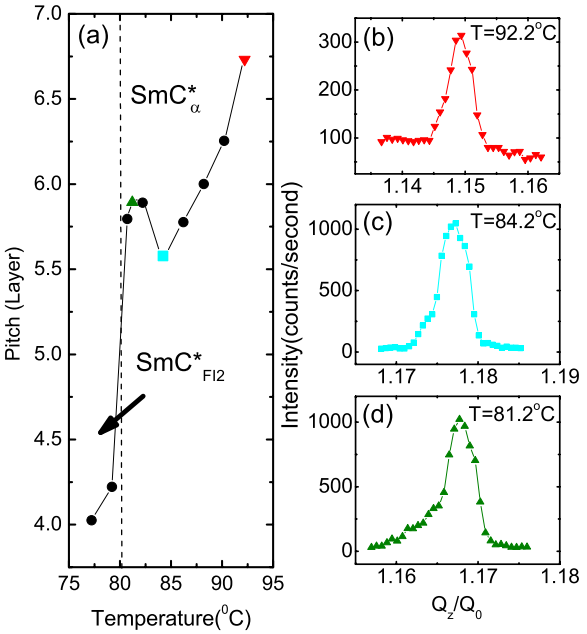

FIG. 5. (Color online) (a) The pitch temperature evolution of the $(73\%\ 10\mathrm{OHF}/27\%\ 11\mathrm{OHF})_{0.85}\ \mathrm{C9}_{0.15}$ ternary mixture in the $\mathrm{Sm}C^*_\alpha$ phase measured by RXRD. [(b)–(d)] Scans of the same mixture at 92.2 °C, 84.2 °C and 81.2 °C.

SmC^*_α to SmC^*_{FI2} transition temperature. Based on the experimental results, the existence of the distorted six-layer phase is unlikely because neither biaxiality nor split peaks are observed. On the other hand, our data cannot rule out the possibility of a small temperature range of a uniaxial phase with sixfold clock arrangement. More experimental results are required to address an important question. What is the difference between a uniaxial phase with a six-layer clock arrangement and an extremum near six layers in the temperature variation of helical pitch in the SmC^*_α temperature window?

IV. CONCLUSION

In conclusion, we have studied binary mixtures of 10OHF and its homologs and found that none of the three homologs stabilize the unusual phase sequence of 10OHF. In most cases, the temperature window of the SmC^*_{FI2} phase continuously decreases with increasing concentration of the doping homologs. In the 10OHF/11OHF/C9 ternary mixtures, the SmC^*_α-SmC^*_{FI2}-SmC^* phase sequence is restored. Our studies show that the SmC^*_{FI2} phase becomes stable in the 10OHF/C9 mixtures but not in both 10OHF/11OHF and 11OHF/C9 binary mixtures. Thus it is surprising to find out that the presence of 11OHF in the ternary mixtures significantly stabilizes the SmC^*_{FI2} phase.

Finally, it is worthwhile to point out that previous studies on the antiferroelectric display are mainly focused on the SmC^*_A phase, which requires a high switching voltage. The SmC^*_{FI2} phase, which is also antiferroelectric, requires much lower E fields to change to the ferroelectric state [2]. Some mixtures studied in this paper with very wide temperature range for the SmC^*_{FI2} phase should be good candidates for research in antiferroelectric displays.

ACKNOWLEDGMENTS

Use of the National Synchrotron Light Source, Brookhaven National Laboratory, was supported by the U.S. Department of Energy, Office of Science, Office of Basic Energy Sciences, under Contract No. DE-AC02-98CH10886. The research was supported in part by the National Science Foundation, Solid State Chemistry Program under Grant No. DMR-0605760. We want to thank Professor P. Barois for lending us the x-ray oven.

[1] R. B. Meyer, L. Liebert, L. Strzelecki, and P. Keller, J. Phys. (Paris), Lett. **36**, L69 (1975).
[2] A. Fukuda, Y. Takanishi, T. Isozaki, K. Ishikawa, and H. Takezoe, J. Mater. Chem. **4**, 997 (1994).
[3] Ch. Bahr and D. Fliegner, Phys. Rev. Lett. **70**, 1842 (1993).
[4] P. M. Johnson, D. A. Olson, S. Pankratz, Ch. Bahr, J. W. Goodby, and C. C. Huang, Phys. Rev. E **62**, 8106 (2000).
[5] P. Mach, R. Pindak, A.-M. Levelut, P. Barois, H. T. Nguyen, H. Baltes, M. Hird, K. Toyne, A. Seed, J. W. Goodby, C. C. Huang, and L. Furenlid, Phys. Rev. E **60**, 6793 (1999).
[6] Z. Q. Liu, S. T. Wang, B. K. McCoy, A. Cady, R. Pindak, W. Caliebe, K. Takekoshi, K. Ema, H. T. Nguyen, and C. C. Huang, Phys. Rev. E **74**, 030702(R) (2006).
[7] L. S. Hirst, S. J. Watson, H. F. Gleeson, P. Cluzeau, P. Barois, R. Pindak, J. Pitney, A. Cady, P. M. Johnson, C. C. Huang, A.-M. Levelut, G. Srajer, J. Pollmann, W. Caliebe, A. Seed, M. R. Herbert, J. W. Goodby, and M. Hird, Phys. Rev. E **65**, 041705 (2002).
[8] A. Cady, J. A. Pitney, R. Pindak, L. S. Matkin, S. J. Watson, H. F. Gleeson, P. Cluzeau, P. Barois, A.-M. Levelut, W. Caliebe, J. W. Goodby, M. Hird, and C. C. Huang, Phys. Rev. E **64**, 050702(R) (2001).
[9] V. Laux, N. Isaert, V. Faye, and H. T. Nguyen, Liq. Cryst. **27**, 81 (2000).
[10] S. T. Wang, Z. Q. Liu, B. K. McCoy, R. Pindak, W. Caliebe, H. T. Nguyen, and C. C. Huang, Phys. Rev. Lett. **96**, 097801 (2006).
[11] K. L. Sandhya, J. K. Song, Yu. P. Panarin, J. K. Vij, and S. Kumar, Phys. Rev. E **77**, 051707 (2008).
[12] W. Weissflog, C. Lischka, S. Diele, I. Wirth, and G. Pelzl, Liq. Cryst. **27**, 43 (2000).
[13] B. K. McCoy, Z. Q. Liu, S. T. Wang, Lidong Pan, Shun Wang, H. T. Nguyen, R. Pindak, and C. C. Huang, Phys. Rev. E **77**, 061704 (2008).
[14] D. A. Olson, X. F. Han, P. M. Johnson, A. Cady, and C. C. Huang, Liq. Cryst. **29**, 1521 (2002).
[15] D. A. Olson, S. Pankratz, P. M. Johnson, A. Cady, H. T. Nguyen, and C. C. Huang, Phys. Rev. E **63**, 061711 (2001).
[16] D. Schlauf, Ch. Bahr, V. K. Dolganov, and J. W. Goodby, Eur. Phys. J. B **9**, 461 (1999).
[17] M. B. Hamaneh and P. L. Taylor, Phys. Rev. Lett. **93**, 167801 (2004).
[18] P. V. Dolganov, V. M. Zhilin, V. K. Dolganov, and E. I. Kats, Phys. Rev. E **67**, 041716 (2003).
[19] M. A. Osipov and M. V. Gorkunov, Liq. Cryst. **33**, 1133 (2006).
[20] Data from films with thicknesses ranging from 100 layers to 250 layers show that the values of Δ_{max}-Δ_{min} in this "six-layer region" are around 0.15°, with major contribution from the surface layers. While for the biaxial SmC^*_{FI2} in the same films, the absolute values of Δ_{max}-Δ_{min} are around 4°.